

MARCH 03 2023

## Measuring vessel underwater radiated noise in shallow water

Alexander O. MacGillivray  ; S. Bruce Martin  ; Michael A. Ainslie  ; Joshua N. Dolman; Zizheng Li; Graham A. Warner



*J. Acoust. Soc. Am.* 153, 1506–1524 (2023)

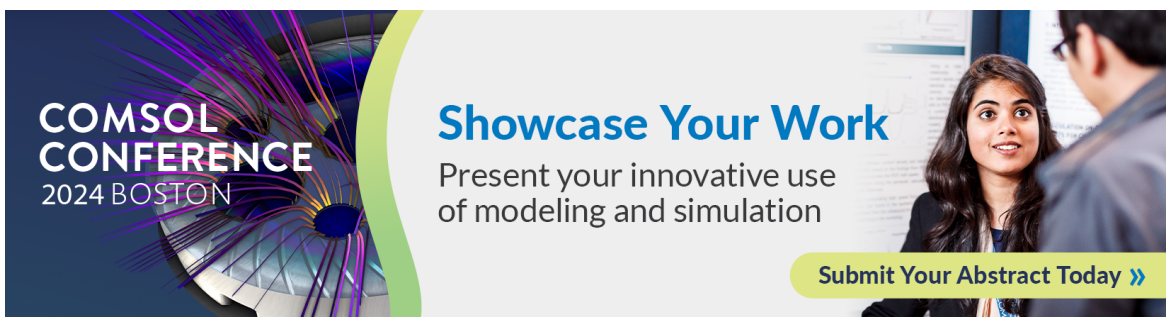
<https://doi.org/10.1121/10.0017433>



View  
Online



Export  
Citation



**COMSOL CONFERENCE**  
2024 BOSTON

Showcase Your Work  
Present your innovative use  
of modeling and simulation

Submit Your Abstract Today »

# Measuring vessel underwater radiated noise in shallow water

Alexander O. MacGillivray,<sup>1,a)</sup>  S. Bruce Martin,<sup>2</sup>  Michael A. Ainslie,<sup>3</sup>  Joshua N. Dolman,<sup>1</sup>  
Zizheng Li,<sup>1</sup> and Graham A. Warner<sup>1</sup>

<sup>1</sup>JASCO Applied Sciences (Canada) Ltd., Victoria, Canada

<sup>2</sup>JASCO Applied Sciences (Canada) Ltd., Halifax, Canada

<sup>3</sup>JASCO Applied Sciences (Deutschland) GmbH, Schwentinental, Germany

## ABSTRACT:

Performing reproducible vessel source level (SL) measurements is complicated by seabed reflections in shallow water. In deep water, with a hydrophone far from the seabed, it is straightforward to estimate propagation loss (PL) and convert sound pressure level (SPL) into SL using the method codified in the international standard ISO 17208-2 [International Organization for Standardization (ISO), Geneva, Switzerland (2019)]. Estimating PL is more difficult in shallow water because of the way that sound reflects from the seabed such that multiple propagation paths contribute to SPL. Obtaining reproducible SL measurements in shallow water requires straightforward and robust methods to estimate PL. From May to July 2021, a field experiment evaluated different methods of measuring vessel SL in shallow water. The same vessels were measured many times in water depths of 30, 70, and 180 m. In total, 12 079 SL measurements were obtained from 1880 vessel transits and 16 hydrophones, distributed across 3 moored vertical line arrays and 2 moored horizontal line arrays. The experiment confirmed that it is possible to obtain reproducible vessel SL estimates in shallow water comparable to within  $\pm 2.5$  dB of ISO-compliant measurements in deep water and repeatable to within  $\pm 1.5$  dB. © 2023 Author(s). All article content, except where otherwise noted, is licensed under a Creative Commons Attribution (CC BY) license (<http://creativecommons.org/licenses/by/4.0/>).

<https://doi.org/10.1121/10.0017433>

(Received 11 October 2022; revised 12 February 2023; accepted 13 February 2023; published online 3 March 2023)

[Editor: Stephen P. Robinson]

Pages: 1506–1524

03 June 2024 18:05:36

## I. INTRODUCTION

Predicting the effects of vessels on the marine ecosystem requires that we model their underwater radiated noise (URN) emissions starting with each vessel's source level (SL). Conceptually, the SL of a vessel is found by measuring its sound pressure level (SPL) as it passes a hydrophone recorder and then adding the propagation loss (PL) to account for the attenuation of the sound between source and receiver. For measurements made in deep water, with a hydrophone far from the seabed, it is relatively straightforward to estimate PL and convert the received SPL into a SL using the method codified in the international standard ISO 17208-2.<sup>1–3</sup> However, many groups interested in the measurement of vessel URN are based in coastal areas where water depths are shallower than the 150 m depth recommended in existing standards. In shallow water, it is more difficult to estimate PL because of the way that sound interacts with the seabed, where multiple propagation paths contribute to the received sound level at a recording location.<sup>4</sup> In shallow water, PL depends on the bathymetry, sound speed profile, and acoustic properties of the seabed at the measurement site. Furthermore, suitable hydrophone geometry must be selected to ensure that reproducible URN measurements are possible. Several choices of PL model and

hydrophone geometry have been proposed,<sup>5–7</sup> but it is unclear what methods are best suited for obtaining reproducible and robust shallow water URN measurements. By robust, we mean that errors in estimated SLs should be insensitive to likely uncertainties in environmental conditions and source-receiver geometry.

To address this knowledge gap, the Transport Canada Innovation Centre (TC-IC) initiated a research project (MMP2) to address the question, “What combination of sensors and analysis methods yield measurements of vessel underwater sound levels in shallow water consistent with those that are known to be accurately obtained in deep water using ISO standard 17208-1/-2?” The project was specifically focused on the measurement of SLs of surface vessels in shallow water. A related source property is radiated noise level (RNL), defined as the sum of SPL and  $20\log_{10}r$  dB, where  $r$  is the source-receiver distance in metres. RNL is straightforward to calculate in deep water (ISO 17208-1, ANSI/ASA S12.64<sup>8</sup>) but is of little practical use in shallow water.<sup>7</sup>

This project was built around a comprehensive field experiment, performed from 5 May through 22 July 2021, that collected a large dataset of vessel URN measurements for a variety of water depths and hydrophone array geometries. Design of the experiment was developed in consultation with the International Organization for Standardization (ISO) working group responsible for the development of

<sup>a)</sup>Electronic mail: alex.macgillivray@jasco.com

ISO 17208 (Underwater acoustics—Quantities and procedures for description and measurement of underwater sound from ships).

To meet the study objectives, the experimental plan called for the same vessel's URN to be measured many times, in different water depths (nominally 30, 70, and 180 m), and with different hydrophone–ship geometries. A local vessel operator in British Columbia's Southern Gulf Islands was identified as a project collaborator and assisted in the planning of hydrophone deployment locations. This operator's vessels were chosen because of their large size and frequent trips, which made it possible to gather a large dataset for statistical analysis since they make repeated passes along the same route many times per day. In August 2020, a review of the study planning white paper with the relevant ISO working group (Technical Committee 43, Sub-Committee 3, Working Group 1)<sup>9</sup> determined the final experimental design, which included the following hydrophone configurations:

- (1) At the deep-water site (180 m), the preferred configuration was a vertical line array (VLA) of three hydrophones so that the measurements are compliant with ISO 17208-1 and 17208-2 (for the measurement of the RNL and SL of a vessel in deep water, respectively). The SL from this location was considered the reference value to be compared to the other locations and hydrophone geometries;
- (2) at the mid-water depth site (70 m), the preferred configurations were two VLAs of three hydrophones at 150 and 350 m from the vessel's nominal track line, as well as a bottom-mounted hydrophone at 121 m from the nominal track line. The latter hydrophone effectively completed a horizontal line array (HLA) when combined with the bottom hydrophones of the two VLAs. Model predictions suggested that water depths of at least 70 m were required to obtain reliable estimates of the SL for frequencies as low as 10 Hz.<sup>7</sup> Measurements close to the vessels and at five times the water depth had predicted advantages for obtaining reliable SLs, which guided the choice of mooring geometries and locations at this site; and
- (3) at the shallow-water site (30 m), the preferred configuration was a HLA of three bottom-mounted hydrophones deployed at horizontal distances of 170, 228, and 344 m from the vessel's nominal track line. This water depth was considered too shallow for a vertical array but is typical of areas such as the Baltic, North, and East China Seas, where future shallow-water measurements are likely to be performed.

In addition, surface-based URN measurements were collected by using a drifting vertical hydrophone array at the beginning, middle, and end of the field experiment. The purpose of collecting vertical array, horizontal array, and drifting array measurements was to compare the variability in SL estimates from the three methods. It was also to compare the complexity of making the measurements and analyzing the data with each method. During the initial array deployments, PL was measured using a controlled acoustic source.

Acoustic inversion methods were applied to the PL data to determine the geoacoustic properties of the seabed at the three measurement sites.

In total, URN data were obtained from a total of 16 hydrophone nodes distributed across 3 moored VLAs, 2 moored HLAs, and a single drifting VLA. Each array had three hydrophones as recommended by the ISO 17208 and ANSI S12.64 standards. This article describes the experimental methods and provides detailed results of the field experiment, including a summary of its findings and conclusions.

## II. BACKGROUND

### A. ISO 17208 and limitations in shallow water

For measurements made in deep water with a hydrophone far from the seabed, the direct and surface reflected paths arrive at hydrophones in the upper half of the water column with more energy than any paths interacting with the seabed. As a result, it is relatively straightforward to account for the two paths and convert the received SPL into a monopole SL without employing numerical acoustic propagation modelling. Measurements of vessel URNs in deep water are codified in ISO standard 17208, Parts 1 and 2, and in ANSI standard S12.64.

ISO 17208 Part 1 and ANSI S12.64 describe procedures for measuring RNL in deep water. This quantity is used by some classification societies to compare with a requirement specification (e.g., for designating silent classes) or to track changes in vessel URN over time. ISO 17208 Part 2 describes a procedure for determining SL in deep water from a RNL measurement. In the existing standards for vessel SL measurement (ISO standards 17208-1, -2, and ANSI S12.64), hydrophone measurements are collected at 15°, 30°, and 45° grazing angles and averaged over repeated passes. On each hydrophone, squared sound pressure must be averaged within a data window defined by a ±30° azimuth angle centered at the closest point of approach (CPA) to the hydrophone for each pass. The intent of these averaging procedures is to smooth out the frequency dependence of the interference between the direct and surface-reflected paths such that the URN measurement is insensitive to minor differences in the source depth and measurement geometry.

ISO 17208-1 requires the use of a hydrophone array whose length is on the order of the vessel length. It implies that the hydrophones are suspended from the surface in some manner. The specification goes on to suggest that bottom-mounted or surface deployed hydrophones could be used, but there is limited guidance on issues that arise with the different options and what must be controlled to obtain a valid measurement. Both types of measurements are challenging. The following are the key constraints essential for URN measurements:

- (1) The location of the hydrophones relative to the vessel must be known to within 10% of the distance (10% range error is equivalent to approximately 0.5 dB bias in SL); and

(2) the measurement platform must not introduce noise levels (NLs) that are above the measured signal in any of the decidecade bands of interest. Possible sources of measurement noise are movement of the hydrophones and sound from the platform that deployed the hydrophones (e.g., engines and hull slap).

Whereas the ISO 17208-1 specification includes data processing steps to address (and correct for) these constraints, it does not provide detailed guidance on the preferred array design or deployment method.

In shallow water, sounds interact with the seabed and multiple paths contribute to the received SPL at a recording location. The number of significant propagation paths depends on the water depth and distance between recorder and vessel; the greater that the distance is, the more paths will contribute significantly to the received level. The amplitude of the seabed reflected paths depends on the incidence angles, seabed composition, and bathymetric profiles. If the seabed composition, speed of sound in the water column, and bathymetry are known, acoustical propagation modelling may be employed to estimate PL and, hence, arrive at the SL.

Measurements in shallow water are not only affected by interactions of the sound with the seabed but also by propagation and sound generation effects that are unique to this environment. Shallow water inhibits the propagation of low frequencies in a manner that depends on the water depth and seabed composition. For some applications, 10 Hz is the minimum frequency of interest; for a typical sand seabed, a 10 Hz cutoff frequency requires a water depth of approximately 65 m.<sup>9</sup> However, there are many places in the world where accessing water deeper than 50 m is logically challenging. For example, much of the North Sea and Baltic Sea, which both have heavy vessel traffic, is less than 40 m deep. Therefore, it is relevant to assess how to make measurements in these shallow areas that are comparable to the accepted deep-water methods.

## B. Terminology and definitions

Developing repeatable (i.e., close when measuring the same thing under the same conditions) and reproducible (i.e., close when measuring the same thing under different conditions) methods for shallow-water URN measurement requires effective communication between stakeholders, which is facilitated by a harmonized and precise terminology with wide acceptance. To this end, we have followed the standard terminology for underwater acoustics specified by ISO 18405.<sup>10,11</sup> We, furthermore, distinguish between abbreviations, such as SPL in text, and symbols, such as  $L_p$ , for equations. Geometrical parameters are defined in Table I. Analysis of sound levels was performed in standard decidecade frequency bands as defined by IEC.<sup>12</sup> These bands are arranged logarithmically and based on powers of ten around a central frequency of 1000 Hz.<sup>13</sup> They are sometimes referred to as “one-third octave” bands because a decidecade is approximately one-third of an octave.

Several URN metrics were evaluated during the MMP2 experiment. The first URN metric of interest for many

TABLE I. Terms and definitions for measurement geometry. All of the quantities are evaluated at the CPA between the source and receiver. The speed of sound in water is  $c_w$ , and the compressional-wave speed in the seabed is  $c_p$ .

Term	Definition	Equation/symbol
Horizontal range	Horizontal distance between source and receiver	$x$
Receiver depth	Vertical distance between sea surface and receiver (i.e., a hydrophone)	$z$
Slant range	Pythagorean distance between source and receiver	$r = \sqrt{x^2 + z^2}$
Grazing angle ( $\theta$ )	Angle below sea surface to receiver at CPA	$\theta = \tan(z/x)$
SCA ( $\psi$ )	Grazing angle at which sound is totally reflected from the seabed	$\psi = \arcsin(c_w/c_p)$ <sup>a</sup>

<sup>a</sup>The critical angle formula provided in this table is only valid for an idealized, homogeneous seabed (i.e., without vertical structure). For the more general case of a stratified seabed composed of elastic layers, the critical angle must be measured or calculated using reflection coefficient formulas for layered media (Ref. 36).

applications is the RNL (symbol  $L_{RN}$ ), which is defined in ISO standard 17208-1,<sup>1</sup>

$$L_{RN} = L_p + 10\log_{10} \frac{r^2}{r_0^2} \text{ dB}, \quad (1)$$

where  $L_p$  is the measured SPL at slant range  $r$ , and  $r_0$  is the standard reference distance of 1 m. The RNL may also be understood as a type of adjusted source level (aSL; see Sec. II D). The RNL was included in the analysis for this project as a reference point for comparisons between methods; however, SL is of greater interest for shallow-water URN measurement. The generic term URN is used to mean any one of SL, RNL, and aSL. These quantities all have the same reference value, which may be written either as  $1 \mu\text{Pa m}$  or  $1 \mu\text{Pa}^2 \text{ m}^2$ , with no material difference in meaning between these two reference values.<sup>11</sup>

## C. SLs

Conceptually, the SL (symbol  $L_S$ ) of a vessel is obtained by adding the SPL (symbol  $L_p$ ) of the vessel, which is measured as it passes a hydrophone recorder, to the PL (symbol  $N_{PL}$ ), which accounts for the attenuation of the sound between source and receiver such that

$$L_S = L_p + N_{PL}, \quad (2)$$

where  $N_{PL}$  may be estimated using numerical acoustic propagation models or through the use of a number of proposed simplified approaches. An estimate of PL is fundamental to calculating SL. Equation (2) follows from the definition of PL, i.e.,

$$N_{PL} \equiv L_S - L_p, \quad (3)$$

and the propagation factor is

$$F = 10^{-N_{PL}/(10 \text{ dB})} \text{ m}^{-2}. \quad (4)$$

The term “spherical spreading” is used to indicate a propagation factor inversely proportional to the square of slant range ( $r$ ),

$$F = r^{-2}. \quad (5)$$

For spherical spreading, PL is given by  $10\log_{10}r^2/r_0^2$  dB.

When a source is close to the sea surface and the receiver is far from other boundaries, the propagation factor includes an additional image-interference term that depends on the grazing angle of the measurement (i.e., the Lloyd’s-mirror effect),

$$F = 4(r \sin(kd \sin \theta))^{-2}, \quad (6)$$

where  $r$  is the slant range,  $\theta$  is the grazing angle, the wave-number is  $k = 2\pi f/c_w$ ,  $f$  is the frequency of interest,  $c_w$  is the speed of sound in water, and  $d$  is the source depth. This model of PL is often appropriate for vessel SL measurements in deep water.<sup>14</sup> In this circumstance, the RNL can be understood as an “affected SL,” which is related to SL by application of a frequency-dependent conversion factor.<sup>4</sup> This is the approach taken by ISO standard 17208–2, which provides a method for correcting the RNL to obtain the SL that is known to be valid in deep water,

$$L_{S,ISO} = L_{RN} + \Delta L_{ISO}, \quad (7)$$

$$\Delta L_{ISO} = -10\log_{10} \frac{14(kd)^2 + 2(kd)^4}{14 + 2(kd)^2 + (kd)^4} \text{ dB}. \quad (8)$$

This formula is based on the interference between the surface-reflected sound and direct path sound, smoothed over frequency, and it is computed from the power average of the propagation factor measured on a VLA at grazing angles of 15°, 30°, and 45° (this is equivalent to averaging the source factor measurement across grazing angles).

In shallow water, the bottom reflected sound also contributes to the received sound pressure, which must be accounted for in the PL. In this circumstance, Eq. (8) no longer holds, and PL must be computed using an alternative method. In this study, four methods of computing the shallow-water PL are compared, as described in Secs. II C 1–II C 4. In each case, the ISO 17208-2 SLs from the deep-water site [ $L_{S,ISO}$ , computed using Eq. (7) and (8)] are used as a reference SL to test how measurements with shallower depths and other URN metrics compare to the accepted standard in deep water.

### 1. SL.HWB (SL by hybrid wavenumber integration and beam tracing method)

Full-wave numerical propagation methods are widely viewed as the reference standard for computing PL in realistic ocean environments.<sup>15</sup> We employed a hybrid propagation model that used a fully elastic wavenumber integration solution up to 4 kHz and a finite-element beam tracing

method above 4 kHz. This is referred to as the hybrid wavenumber integration and beam tracing (HWB) method,

$$L_{S,HWB} = L_p + N_{PL,HWB}. \quad (9)$$

In decideade bands at 4 kHz and below, PL was calculated using the VSTACK wavenumber integration model,<sup>15</sup> and in decideades above 4 kHz, PL was calculated using the BELLHOP beam tracing model.<sup>16</sup>

VSTACK computes PL versus depth and range for arbitrarily layered, range-independent, acoustic environments using the wavenumber integration approach to solve the exact (range-independent) acoustic wave equation. This model is valid over the full angular range of the wave equation and can account for the elasto-acoustic properties of the sub-bottom. VSTACK computes sound propagation in arbitrarily stratified water and seabed layers by decomposing the outgoing field into a continuum of outward-propagating plane cylindrical waves. Seabed reflectivity in the model is dependent on the seabed layer properties: compressional and shear-wave speeds, attenuation coefficients, and layer densities.

BELLHOP computes PL versus range and depth using the finite-element beam tracing method, which is a variant of the ray-trace method.<sup>15</sup> Although BELLHOP is a fully range-dependent propagation model, only range-independent predictions were used for the current application. Bottom loss was included in the BELLHOP model by using tabulated, frequency-dependent reflection coefficients for a layered elastic seabed, which were generated using the reflectivity method (i.e., as in VSTACK). Attenuation of acoustic energy by molecular absorption in seawater was accounted for with frequency-dependent absorption coefficients. Both numerical models assumed iso-velocity sound speed profiles in the water column and fully elastic, vertically stratified geoacoustic profiles in the seabed (see Sec. III B for a justification of iso-velocity modelling). Seabed geoacoustic properties at each site were based on inverted properties (Sec. IV B). The PL in each decideade band was calculated from the mean propagation factor calculated at 50 frequencies, which were spaced logarithmically between the minimum and maximum decideade band limits. The environment was assumed to be range-independent for all of the PL calculations with constant water depth at each site.

For this study,  $N_{PL,HWB}$  was calculated at a single source depth under the simplifying assumption that the vessel itself is a point-like source of sound. However, the point-source assumption is not the only available choice when using this method. Indeed, several past studies have calculated vessel URN with full-wave methods under the assumption that the source of radiation is not point-like but is, instead, distributed with depth. One common assumption is to apply an incoherent depth-averaging technique whereby  $N_{PL,HWB}$  is calculated assuming a normal distribution of source depths.<sup>17–19</sup> While the assumption of a vertically distributed source may result in a more robust SL estimate, as originally demonstrated by Wales and Heitmeyer,<sup>17</sup> depth

averaging has not been used for calculating  $N_{PL,HWB}$  in the current study because there exists no widely agreed-on approach for applying this technique.

## 2. SL.ECA (SL by ECHO certification alignment method)

In shallow water, it is unlikely that measurements will be made at a grazing angle of  $30^\circ$ . The ECHO certification alignment (ECA) project, as reported by Ainslie *et al.*,<sup>7</sup> applied an alternative formula to Eq. (8) that is valid for any grazing angle. This alternative formula, which is reproduced here, accounts for the influence of the sea surface on sound propagation but does not include energy reflecting from the seabed,

$$L_{S,ECA} = L_{RN} - \Delta L_{ECA} + \Delta L_\alpha, \quad (10)$$

$$\Delta L_{ECA} = 10\log_{10}\gamma \text{ dB}, \quad (11)$$

where  $\gamma$  is the dipole to monopole conversion factor, which is shown in Eq. (12) as a function of grazing angle,  $\theta$ ,

$$\gamma(\theta) = 2 - \frac{\sin(2\pi Tf_2) - \sin(2\pi Tf_1)}{\pi T(f_2 - f_1)}; \quad T = \frac{2d\sin\theta}{c_w}. \quad (12)$$

Here,  $f_1$  and  $f_2$  are the lower and upper frequencies, respectively, of the decidecade being analyzed,  $d$  is the depth of the source, and  $c_w$  is the speed of sound in water. This approach includes an absorption factor,  $\Delta L_\alpha$ , which accounts for sound energy lost to seawater across the slant range.<sup>20</sup> Note that the same definition of  $\Delta L_\alpha$  is applied to SL.SCA and SL.M-A, below.

## 3. SL.SCA (SL by the seabed critical angle method)

By accounting for contribution of the seabed to PL, a more general version of the approximation employed in ISO 17208–2 may be obtained, which includes a term for the bottom reflection via the seabed critical angle (SCA), as well as an explicit term for the direct path arrival,

$$L_{S,SCA} = L_{RN} - \Delta L_{SCA} + \Delta L_\alpha, \quad (13)$$

$$\Delta L_{SCA} = 10\log_{10}\left(\sigma_1 + \frac{\psi r}{H}\sigma_\psi\right) \text{ dB}, \quad (14)$$

where  $r$  is the slant range from the source to receiver,  $H$  is the water depth, and  $\psi$  is the SCA. The correction terms for the interference between the direct path and the surface reflection ( $\sigma_1$ ) and the interference between the direct path and the seabed reflection ( $\sigma_\psi$ ) are given by

$$\sigma_1 \approx \left(\frac{1}{2} + \frac{1}{4\eta\sin^2\theta}\right)^{-1}; \quad \eta = k^2 d^2, \quad (15)$$

and

$$\sigma_\psi \approx \left(\frac{1}{2} + \frac{3}{4\eta\sin^2\psi}\right)^{-1}. \quad (16)$$

The grazing angle,  $\theta$ , and critical angle,  $\psi$ , are as specified in Table I.

The  $\Delta L_{SCA}$  formula is an empirical combination of two different expressions, valid in the high- and low-frequency limits, respectively. The high-frequency (incoherent) propagation factor can be written as a combination of spherical spreading at short range and cylindrical spreading at long range such that

$$F_{HF} = \frac{2}{r^2} + \frac{2}{rH} \int_0^\psi d\theta, \quad (17)$$

$$F_{HF} = \frac{2}{r^2} + \frac{2\psi}{rH}. \quad (18)$$

The low-frequency formula is obtained by replacing the factor of 2 in Eq. (17) with  $4\sin^2(kd\sin\theta)$  and integrating the cylindrical spreading term over angle

$$F_{LF} = \frac{4\sin^2(kd\sin\theta)}{r^2} + \frac{1}{rH} \int_0^\psi 4\sin^2(kd\sin\theta)d\theta. \quad (19)$$

Assuming  $kd \ll 1$  and correcting a factor of 4 error in the dipole correction from Ainslie *et al.*,<sup>21</sup> the low-frequency result is

$$F_{LF} = \frac{4\eta\sin^2\theta}{r^2} + \frac{4\psi\eta\sin^2\psi}{3rH}. \quad (20)$$

$F_{SCA}$  is then an empirical combination of  $F_{LF}$  and  $F_{HF}$  such that

$$F_{SCA} = \frac{\sigma_1 + \frac{\psi r}{H}\sigma_\psi}{r^2}, \quad (21)$$

which simplifies to Eq. (18) at high frequency and simplifies to Eq. (20) at low frequency. Including an absorption term, Eq. (13) then follows by using

$$L_{S,SCA} = L_p + 10\log_{10}\frac{F^{-1}}{r_0^2} \text{ dB}, \quad (22)$$

where the reference range is  $r_0 = 1 \text{ m}$ . Numerical comparisons show that PL calculated using Eq. (20) is in good agreement with more exact methods (Fig. 1).

## 4. SL.M-A (SL by the Meyer and Audoly method)

Meyer and Audoly (M-A)<sup>22</sup> proposed an empirical formula to correct RNL, which is measured on a vertical array of hydrophones, for the influence of multiple reflections on the sea surface and seafloor in shallow water to obtain SL. Their empirical formula was developed using numerical simulations performed for a variety of measurement conditions, sound speed profiles, and seafloor compositions. The correction factor is shown in Eq. (24), where  $Q = 0.75$ ,  $i^2 = -1$ ,  $d$  is the depth of the source, and  $c_w$  is the speed of sound in water. The correction factor is formulated as a second-order high-pass filter, where the correction factor is

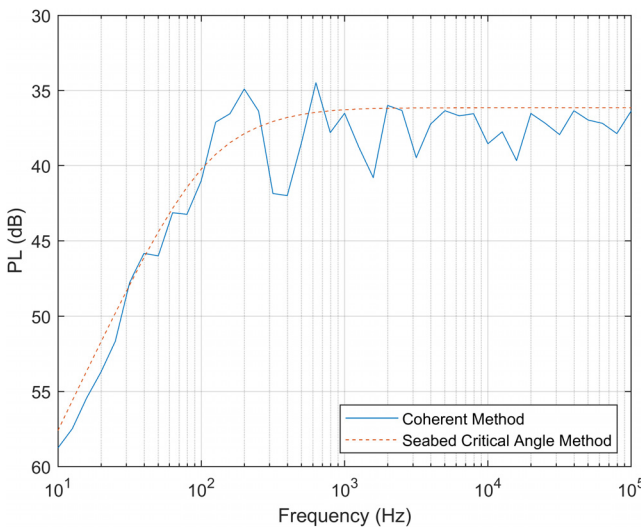


FIG. 1. (Color online) Comparison of PL re  $1\text{ m}^2$  versus frequency for a sand seabed, calculated using coherent images (solid line) and the SCA method (dashed line). The coherent PL curve was calculated using formulas from Ainslie and Wood (Ref. 38). The parameters for the calculation were as follows: 5 m source depth, 20 m receiver depth, 30 m water depth, 200 m horizontal range, water sound speed 1500 m/s, seabed sound speed 1796 m/s, and seabed density ratio 2.086.

constant above the cutoff frequency,  $f_0$ , and follows a constant increase of 20 dB per decade band below  $f_0$  such that

$$L_{S,M-A} = L_{RN} - \Delta L_{M-A} + \Delta L_\alpha, \quad (23)$$

$$\Delta L_{M-A} = 10 \log_{10} \left| \frac{\varepsilon K}{\frac{f_0^2}{f^2} + \frac{i f_0}{Q f} - 1} \right| \text{dB}; \quad f_0 = \frac{c_w}{2\pi d}, \quad (24)$$

where  $K$  represents the influence of sound energy at high frequency due to sea surface reflections, and  $\varepsilon$  represents the influence of additional reflections on the seafloor.

$$\varepsilon = \begin{cases} 1 & \text{if the seafloor is considered soft,} \\ 2 & \text{if the seafloor is considered hard,} \end{cases} \quad (25)$$

$$K = 2 \max \left( \sqrt{\frac{x}{H}}, 1 \right), \quad (26)$$

where  $x$  and  $H$  are as defined in Table I. In the case of a hard seafloor, such as basalt, this factor represents a doubling of sound energy. This method was specifically developed for three channel hydrophone arrays, thus, SL.M-A has only been applied to array-averaged RNL measurements to be consistent with the intended methodology.

#### D. aSLs and RNL

The previously discussed URN metrics model the vessel sound field as a monopole point source at a source depth,  $d$ . The aSL, instead, models the vessel sound field as a dipole consisting of the point source and its image reflected by the sea surface. Although it is unsuitable for modelling sound

propagation (for which SL is better suited), this method is useful for direct comparisons of URN between vessels, between a vessel and an URN requirement, or between measurements in different circumstances of the same vessel. This is closely related to RNL in deep water and replaces RNL in shallow water. Equations (27) and 28 show the adjustment to be applied to each SL metric,<sup>23</sup>

$$L'_S = L_S + \Delta L_S, \quad (27)$$

$$\Delta L_S = 10 \log_{10} \frac{14(kd)^2 + 2(kd)^4}{14 + 2(kd)^2 + (kd)^4} \text{ dB}, \quad (28)$$

where the adjustment is evaluated at a grazing angle of 30°. Interestingly, this adjustment is the inverse of the ISO 17208–2 correction [Eq. (8)].

### III. METHODS

#### A. Experimental design

It was determined during the development of the experimental design that to understand the variability of shallow-water measurements relative to those performed in deep water, the same vessel's URN would be measured many times, in different water depths, and with different measurement geometries. A local operator collaborated with the project by supporting measurements of their vessels along a frequently transited route between Tsawwassen and Swartz Bay. The operator instructed the crew to transit past the hydrophone arrays and provided voyage logs for three of their vessels (Table II). The logs contained the following information for each voyage:

- Number of passengers aboard;
- departure and arrival time; and
- fore and aft draft.

The identities of these vessels have been anonymized, and they are henceforth referred to as vessels A, B, and C.

The identity, position, and speed over ground of vessels A–C were obtained from the automatic identification system (AIS). A total of 2732 vessel passes were recorded at the 3 test sites during the field measurement period (Table III). Following a manual quality review to exclude unsuitable measurements, a total of 1880 vessel passes were accepted for subsequent analysis (see Sec. III C for acceptance criteria). The measurement acceptance rate of approximately 70% exceeded expectations despite the relatively high traffic volume in the study area and opportunistic nature of the measurement schedule. Each individual vessel pass resulted in multiple URN measurements because multiple hydrophone nodes were deployed at each site.

URN measurements were performed at three locations with nominal water depths of 30, 70, and 180 m (Fig. 2). The deep site (180 m) served as the reference deep-water location for comparison to the shallow-water sites. The intermediate site (70 m) met the 65 m minimum criterion for acceptable acoustic propagation at 10 Hz (see Sec. II A). The shallow-water site (30 m) did not meet the criterion but had a typical

TABLE II. Vessel design specifications. The identities of the vessels have been anonymized. CPP, controllable-pitch propeller; RPM, revolutions per minute.

Vessel	Length (m)	Breadth (m)	Propeller type	Propeller diameter (m)	Blades per propeller	Nominal propeller RPM	Installed power (kW)	Drive type
A	167	27	Twin screw CPP	3.4	4	210	15 600	Diesel/LNG
B	167	27	Twin screw CPP	3.4	4	210	15 600	Diesel/LNG
C	160	28	Single screw CPP	5.0	4	140	16 000	Diesel-Electric

water depth for measurements made in shallow continental shelf areas and, hence, was relevant for informing international standards. The bathymetry at the shallow site was sloping along the vessel track but relatively flat across-track. The bathymetry at the intermediate site was flat all around the site. The deep site was in a bowl that rose to 160 m depth  $\sim$ 1 km from the measurement site in all directions.

## B. Apparatus

Moored hydrophones were deployed for this study from 5 May to 22 July 2021. The moored hydrophone arrangement consisted of three VLAs and two HLAs (Fig. 3). The three vertical arrays were referred to as D.VLA.150, I.VLA.150, and I.VLA.350. At the intermediate site, the bottom hydrophone of the two VLAs and the baseplate at 121 m from the nominal track line were combined to form a horizontal array, which is referred to as I.HLA.121. At the shallow site, the three baseplate hydrophones were combined to form a horizontal array, which is referred to as S.HLA.170. The actual locations and depths of the hydrophone elements, which differed slightly from the planned arrangement, were recorded by the field team following deployment of the moored hydrophones (Table IV). The three vertical arrays incorporated depth loggers at the location of the top-most hydrophone, which were used for measuring array knock-down due to tidal currents.

All of the moored hydrophones were sampled continuously using AMAR G4 acoustic recorders (JASCO Applied Sciences, Victoria, British Columbia, Canada) at 128 kHz sampling rate. All of the hydrophones were GeoSpectrum model M36-V35 sensors (Dartmouth, Nova Scotia, Canada) with a nominal sensitivity of  $-164$  dB re 1 V/ $\mu$ Pa. Each hydrophone was provided with a factory calibration curve by the manufacturer, which was verified in the laboratory by JASCO through formal qualification testing. Furthermore, the hydrophones were calibrated prior to deployment and on retrieval using a

G.R.A.S 42AC pistonphone calibrator (Holte, Denmark) at 250 Hz. The real-time clocks on all of the hydrophone recorders were synchronized with Global Positioning System (GPS) time prior to deployment. The maximum clock drift for the deployment period was estimated at 52 s. The coordinates of the moorings at the seabed were localized to within  $\pm 1.5$  m (RMS) accuracy by range-fixing their positions from the surface using EdgeTech PORT-LF and SPORT-LF acoustic release units (West Wareham, MA).

A limited number of additional URN measurements were performed using a drifting vertical array of hydrophones, suspended from an auxiliary vessel, which is the suggested sensor configuration for ISO 17208–1/-2 compliant measurements in deep water. These measurements were collected at the shallow, intermediate, and deep sites on three separate occasions throughout the experiment period. The overall quality of measurements from the drifting array was poorer than the measurements from the static moorings. This was partly due to increased self-noise, which was caused by wave-induced surface motion and currents, and partly due to difficulties in controlling the measurement geometry, which was caused by the relative motion of the source vessel and measurement vessel. Thus, the drifting hydrophone data were not used for evaluation of the different SL metrics (see Sec. IV) as they were limited in number and generally of poorer quality than the moored hydrophone data.

Profiles of water temperature and salinity were collected throughout the trials using a Minos-X (AML Oceanographic, Victoria, British Columbia, Canada) conductivity-temperature-depth (CTD) probe. The profiles from the CTD probe were used to calculate sound speed profiles for each month and site during the experiment. Water sound speeds varied from 1480 to 1490 m/s during the experiment with mean speed gradually increasing over time due to warming water. The CTD data suggested that sound speed profiles were weakly stratified with depth during the experiment and would, thus, have negligible influence on URN measurements. Numerical tests, undertaken to investigate this assumption, indicated that there was no significant difference between PL calculations performed using actual measured profiles and iso-velocity profiles when the receiver range was less than 1 km. Therefore, it was concluded that the iso-velocity approximation was valid for calculating vessel SLs from the experimental data.

## C. URN data analysis

To obtain URN measurements for each vessel pass, the hydrophone recordings were analyzed with ShipSound, a

TABLE III. Number of vessel transits measured at each site during May, June, and July 2021. The number accepted indicates how many transits had one or more URN measurements that passed a manual data-quality review.

Vessel	Median speed [kn (m/s)]	Median draft (m)	Transits measured (accepted)		
			Deep	Intermediate	Shallow
A	20.1 (10.3)	4.6	434 (239)	384 (206)	372 (261)
B	19.3 (9.9)	4.4	541 (398)	269 (253)	359 (266)
C	20.1 (10.3)	5.5	114 (73)	128 (77)	131 (107)

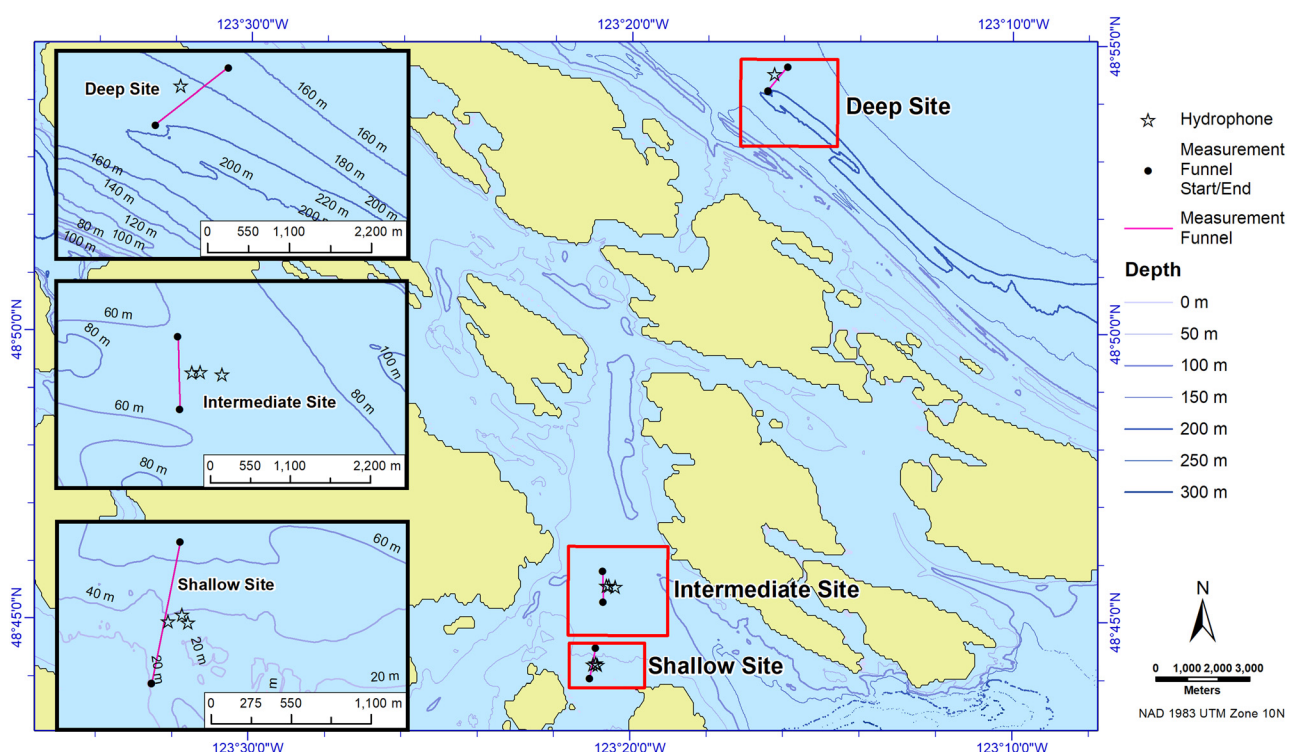


FIG. 2. (Color online) Map of hydrophone deployment locations in the British Columbia Salish Sea for vessel URN recording and analysis. The shallow and intermediate sites were located in Swanson Channel between Salt Spring and North Pender Islands. The deep site was located in Georgia Strait, near the entrance of Active Pass.

component of JASCO's custom vessel noise measurement system, PortListen® (Victoria, British Columbia, Canada). ShipSound automatically tracks the identity, position, and speed over ground of vessels transiting past the hydrophone arrays using the AIS. Any AIS vessels transiting through a  $1\text{ km} \times 4\text{ km}$  measurement funnel around each measurement site were automatically analyzed by ShipSound to obtain an URN measurement. Environmental conditions (wind speed

and current speed) and the coordinates of nearby AIS vessels were also recorded for each automated measurement.

ShipSound computed RNL and SL.HWB within a data window defined by a  $\pm 30^\circ$  azimuth angle centered from the CPA to the hydrophone. For acoustic data within the measurement window, ShipSound analyzed acoustic data in decidecade frequency bands from 10 Hz to 63 kHz. Each sound recording was processed using 1-s sliding fast Fourier

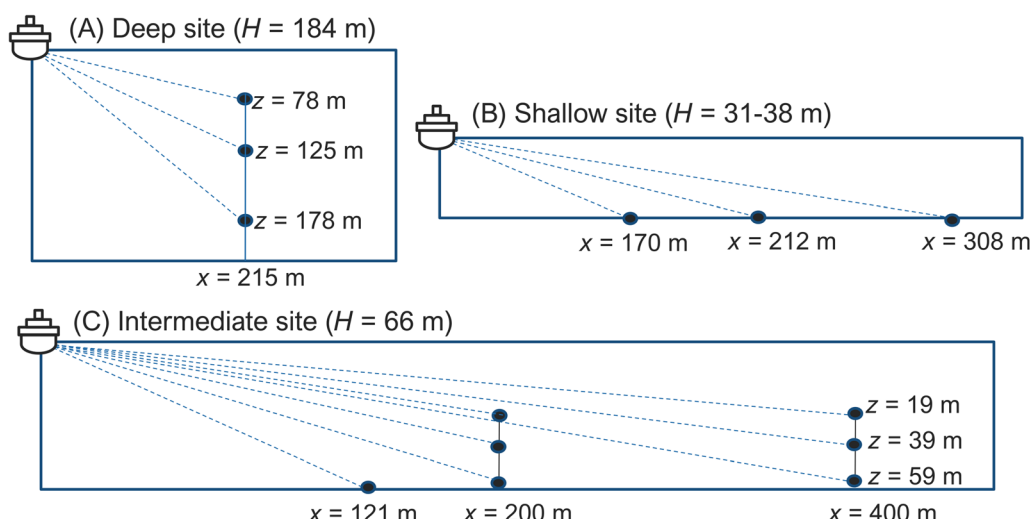


FIG. 3. (Color online) As-deployed measurement geometries for MMP2 data collection in 2021. Dots represent the hydrophone nodes. Horizontal distance ( $x$ ) indicates nominal CPA distance of the mooring from the planned vessel track—note that actual CPA distances varied between vessel transits. Receiver depth ( $z$ ) indicates hydrophone node depths below the sea surface on the vertical arrays. Water depth ( $H$ ) indicates mean low-tide water depth at chart datum.

TABLE IV. As-deployed hydrophone geometry and mooring coordinates for URN data collection. The water depth at each site is the Canadian Hydrographic Service (CHS) NONNA-10 CHS (Ref. 37) surveyed water depth at the deployment location (mean low-tide reference). The depth below sea surface for each hydrophone element is the nominal value calculated from the water depth, assuming the array is oriented vertically in the water column.

Site	Mooring type	Mooring identification	Longitude	Latitude	Depth below sea surface (m)			
					Element 1	Element 2	Element 3	Water depth (m)
Deep	VLA	D.VLA.150	123° 16' 14.9697" W	48° 54' 30.8389" N	77.5	124.6	177.6	184.2
Intermediate	VLA	I.VLA.150	123° 20' 33.2397" W	48° 45' 37.5228" N	19.0	39.1	59.1	65.7
		I.VLA.350	123° 20' 23.5431" W	48° 45' 36.5146" N	19.4	39.4	59.5	66.1
Shallow	Base plate	I.BP.121	123° 20' 37.0585" W	48° 45' 37.5060" N	65.4	—	—	65.9
		S.BP.170	123° 20' 51.0784" W	48° 44' 15.0527" N	30.8	—	—	31.3
		S.BP.228	123° 20' 53.1136" W	48° 44' 16.8535" N	37.2	—	—	37.7
		S.BP.344	123° 20' 57.8190" W	48° 44' 15.3470" N	36.8	—	—	37.3

transforms (FFTs) using a power-normalized Hann window and 50% overlap, to obtain power spectral density (PSD) levels versus time. Vessel track information was obtained from AIS data. Because the AIS transmitter/receiver was not necessarily coincident with the vessel's acoustic source, the acoustic CPA was determined by tracking the range and speed of the source using an automated tracking algorithm based on the cepstrogram method.<sup>24</sup> The automated CPA time was verified (and adjusted if necessary) during manual quality review by a human analyst. The RNL and SL.HWB values were computed as the decibel level of the mean source factor from the RNL and SL.HWB data from all of the 1-s sample locations along the vessel track within the ±30° data window [i.e., see ISO 17208–1:2016, Eq. (8)]. Background

noise SPLs were computed by averaging measured sound levels over two 1-min intervals: 1 min just before the vessel entered the entrance funnel and 1 min after it left the exit zone. Measured SPL was compared with the NL in decidecade frequency bands and adjusted if  $3 \text{ dB} \leq \text{SPL} - \text{NL} < 10 \text{ dB}$ , according to the method prescribed in the ISO 17208-1 standard (even though the method leads to an undesirable step change of 0.5 dB in SL). Decidecade band levels were discarded when  $\text{SPL} - \text{NL} < 3 \text{ dB}$ .

In all instances, array-average values (i.e., for the HLA and VLA measurements) were computed from the power-mean value of the three individual hydrophone nodes, according to the method prescribed by ISO standard 17208-1,

$$L_X = 10 \log_{10} \left[ \frac{10^{L_X(h_1)/(10 \text{ dB})} + 10^{L_X(h_2)/(10 \text{ dB})} + 10^{L_X(h_3)/(10 \text{ dB})}}{3} \right] \text{ dB}, \quad (29)$$

where  $L_X$  was the array-average value of RNL or SL, and  $L_X(h_n)$  was the single-node measurement from hydrophone,  $n$ . In some cases, a single-hydrophone measurement was excluded from the array-average value if it was rejected following a manual data-quality review.

Each automated URN measurement from ShipSound was subjected to a manual quality review by a human analyst. For each measurement, the analyst inspected the vessel track, spectrogram, background NLs, received levels, and SLs recorded by ShipSound. Measurements were rejected under the following circumstances:

- (1) Other AIS vessels were present within four times the measured CPA of the vessel of interest;
- (2) spectrograms visibly contained contaminating noise from sources other than the vessel of interest (including non-AIS vessels);
- (3) measurements had three or more decidecade bands with SPL equal to NL in the range 50–1000 Hz;
- (4) pressure waveforms contained clipped samples inside more than six 1-s intervals inside the data window; and

(5) vessel AIS tracks had an unsteady speed or heading in the measurement window.

In addition, measurements on the vertical arrays were automatically rejected when data from the depth loggers indicated that knock-down due to tidal currents was sufficient to introduce >10% error in the CPA estimate, as suggested by ISO 17208-1.

## IV. RESULTS

### A. Measurement summary

From the experimental data, ShipSound automatically analyzed a total of 12 079 unique URN measurements on 16 individual hydrophone nodes for vessels A–C. Of this total, 7675 measurements passed a manual data quality review. Speeds of the vessels varied during the experiment, but most URN measurements were collected at speeds between 17 and 22 kn (8.8–11.3 m/s) with a mixture of port and starboard aspects for each vessel. The routes of the vessels also varied during the experiment and, thus, URN measurements

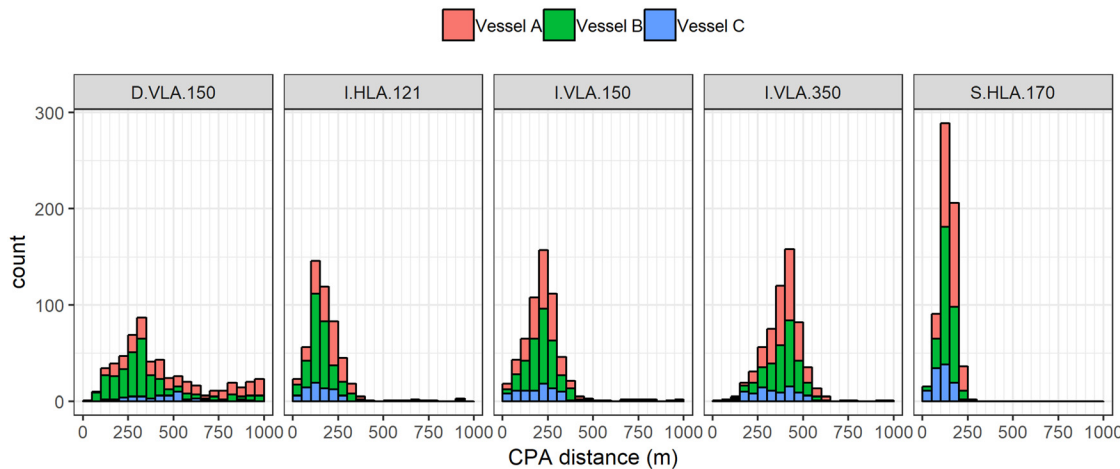


FIG. 4. (Color online) Histogram of vessel CPA horizontal distance ( $x$ ) to each hydrophone array for accepted URN passes. CPA distances for the horizontal arrays are referenced to the closest hydrophone to the vessel track.

were sampled at a range of horizontal CPA distances, out to a maximum distance of 1 km (Fig. 4). Reference SLs (Sec. IV C) were calculated using a subset of the measurements from the deep site that conformed most closely to the ISO 17208–1 measurement procedure.

An initial analysis of SL data from ShipSound indicated that the URNs of vessels A–C were strongly dependent on speed through water at the time of measurement (see Sec. IV C). All three vessels exhibited a *U*-shaped trend of SL versus speed through water with minimum sound emissions in the 17–19 kn (8.8–9.8 m/s) range. This type of SL-versus-speed curve is characteristic of controllable-pitch propellers, which were used on all three vessels.<sup>25,26</sup> The mean draft of the vessels did not vary substantially over the course of the experiment, and variations in vessel trim did not appear to have a significant influence on measured SLs.

## B. Inverted seabed properties

Characterization of the sound propagation properties at the three measurement sites was a key input to the vessel SL analysis. A nonlinear Bayesian inversion algorithm was applied to calibrated measurements of PL versus source-receiver range at the deep, intermediate, and shallow URN measurements sites.<sup>27</sup> The result of the algorithm was a set of geoacoustic profiles (referred to as the maximum *a posteriori*, or MAP, estimates), describing the elastic properties of the seabed materials versus depth below the seafloor (Table V). An inversion study by Pignot and Chapman,<sup>28</sup> performed approximately 15 km southeast of the intermediate site, yielded similar compressional-wave speed estimates in the surface sediment (1605–1720 m/s) and basement layers (2160–2368 m/s) but larger estimates of the surface layer thickness (50–75 m).

The MAP geoacoustic profiles were used as input to the VSTACK and Bellhop full-wave propagation models (see Sec. II C 1) for calculating vessel SLs in ShipSound using the HWB method. The MAP profiles were also used to determine the SCA ( $\psi$ ) versus frequency (Fig. 5) and  $\varepsilon$  value

for calculating vessel SLs using the SCA and M-A methods, respectively.

## C. Reference SLs

Reference SLs for vessels A–C were obtained from URN measurements on the deep VLA and analyzed according to the procedure from ISO standard 17208–2. For each vessel pass, array-average SLs were computed from the power-mean values of the VLA nodes [Eq. (29)]. SL measurements were then binned by speed through water in 1 kn (0.51 m/s) bins, filtered by CPA distance, and arithmetically averaged to compute reference decidecade band SLs (Fig. 6). Inspection of the reference measurements suggested that SLs of vessels A–C were most repeatable in the 20–21 kn (10.3–11.3 m/s) speed range and in frequency bands above 100 Hz.

The reference measurements were filtered by CPA distance before averaging such that the mean range conformed

TABLE V. Estimated geoacoustic parameters versus depth below seafloor for the deep, intermediate, and shallow sites based on the MAP inverted models. Shear-wave speed and attenuation were only estimated for the top sediment layer.  $c_p$ , compressional-wave speed;  $\rho$ , density;  $\alpha_p$ , compressional-wave attenuation;  $c_s$ , shear-wave speed;  $\alpha_s$ , shear-wave attenuation.

Depth below seafloor (m)	$c_p$ (m/s)	$\rho$ (g/cm <sup>3</sup> )	$\alpha_p$ (dB/λ)	$c_s$ (m/s)	$\alpha_s$ (dB/λ)
Deep site					
0–2.8	1460–1466	1.32–1.33	0.80–0.12	260	0.61
>2.8	2496	2.47	0.47		
Intermediate site					
0–2.9	1545–1549	1.82	1.00–0.97	40	2.59
2.9–4.9	1565–1637	1.86–1.91	0.10–0.03		
4.9–10.3	1942–1970	2.00–2.20	0.02–0.03		
>10.3	2238	2.45	0.81		
Shallow site					
0–1.4	1480–1488	1.61–1.63	0.86–0.13	94	2.10
1.4–13.2	1838–2261	2.29–2.44	0.02–0.07		
>13.2	2401	2.46	0.97		

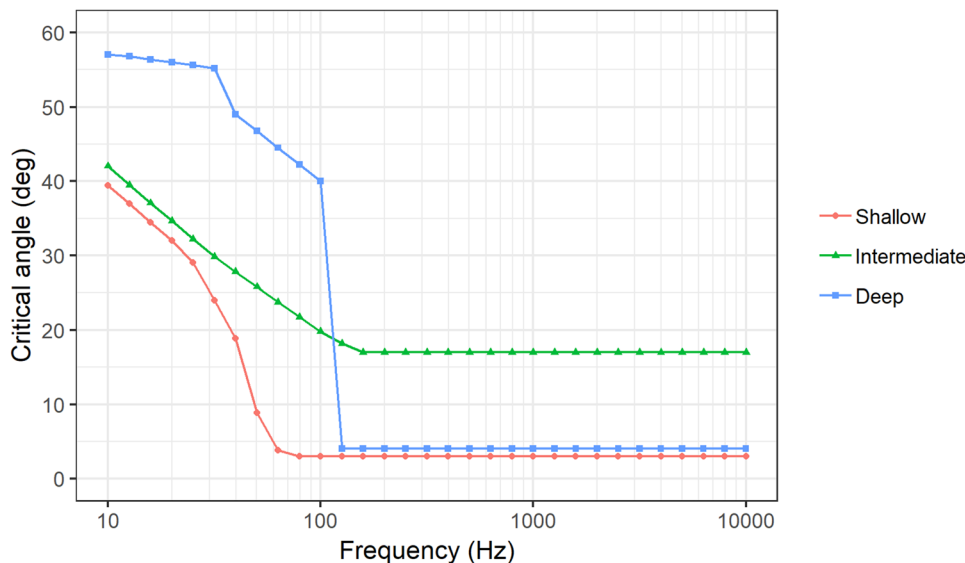


FIG. 5. (Color online) Estimated SCA ( $\psi$ ) versus frequency by measurement site. The  $\psi$  value in each frequency band was estimated from the magnitude of the seabed reflection coefficient versus grazing angle,  $|R(\theta)|$ , which was calculated numerically from the MAP inverted geoacoustic model (Table V) using the plane wave reflection coefficient (Ref. 15). The critical angle in each frequency band was taken to be the smallest grazing angle at which the reflection loss passed 3 dB.

as closely as possible to the measurement angles specified by ISO standard 17208–1 (Table VI). At the deep VLA, a CPA distance of 215 m yielded nominal measurement angles of 20°, 30°, and 40°. While this was a slightly narrower range of angles than those specified by the ISO

standard (15°, 30°, and 45°), this difference was not expected to significantly affect the quality of the reference measurements. After filtering, reasonable conformance with the ISO geometry was possible for vessels A and B but not for vessel C because it consistently passed too far from the

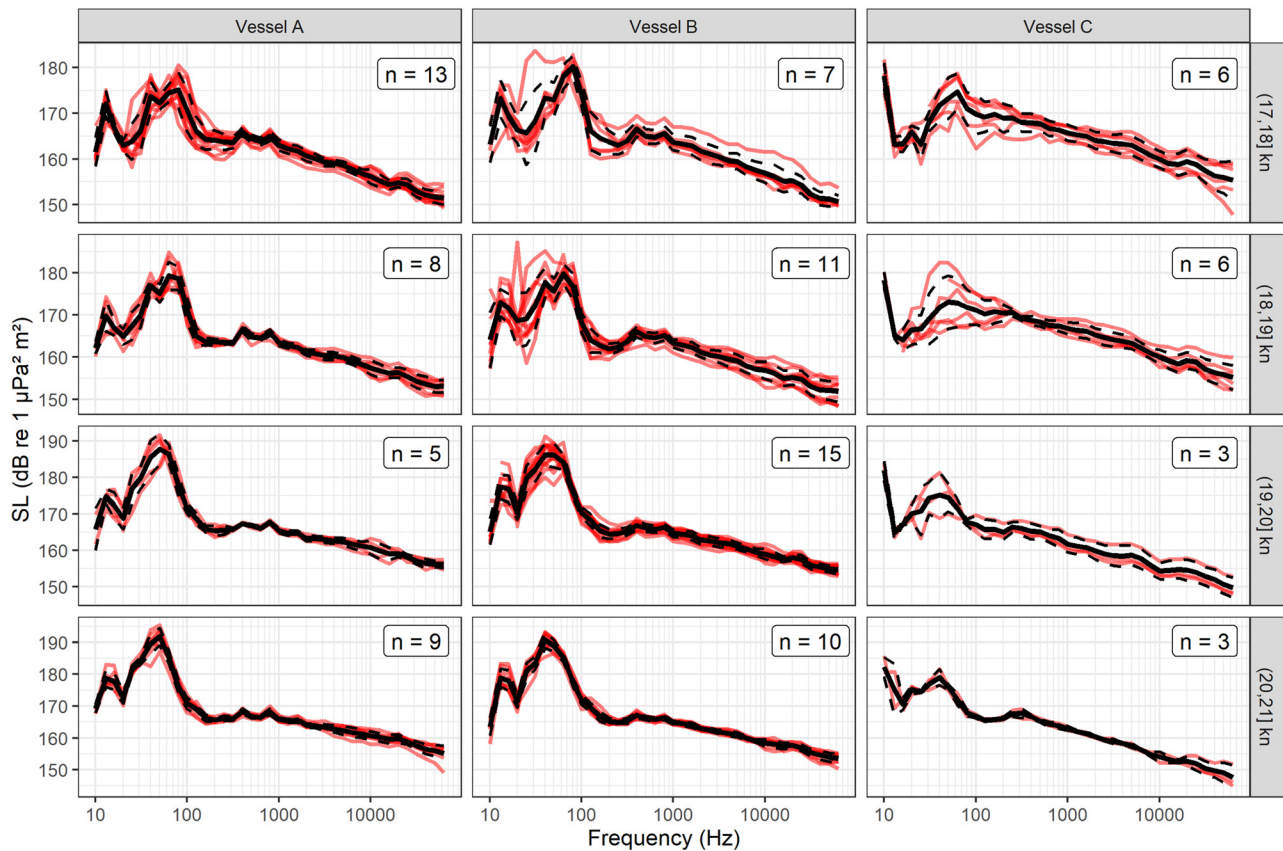


FIG. 6. (Color online) Reference SLs for vessels A–C (columns) computed in 1 kn (0.51 m/s) speed through water bins (rows) from VLA measurements at the deep site. Measurements for vessel A were filtered between 100 and 300 m horizontal CPA distance to the VLA. Measurements for vessel B were filtered between 150 and 250 m horizontal CPA distance to the VLA. Measurements for vessel C were filtered between 50 and 450 m horizontal CPA distance to the VLA. Red lines, individual array-average measurements; solid black line, arithmetic mean value; dashed black line, standard deviation. The  $n$  values indicate the number of individual array-average measurements contributing to the mean. Mean and standard deviation CPA distances for these measurements are provided in Table VI.

TABLE VI. Mean ( $\pm$  standard deviation) CPA distances to the deep VLA for reference SL measurements of vessels A–C (see Fig. 6).

Speed through water bin (kn)	CPA (m)		
	Vessel A	Vessel B	Vessel C
17–18	226 $\pm$ 61	213 $\pm$ 24	265 $\pm$ 89
18–19	221 $\pm$ 33	203 $\pm$ 30	286 $\pm$ 43
19–20	219 $\pm$ 70	193 $\pm$ 30	373 $\pm$ 44
20–21	215 $\pm$ 65	210 $\pm$ 23	343 $\pm$ 121

VLA (see Table VI). This suggests that reference SLs for vessel C were of a lower grade than those of the other two vessels. Therefore, reference SLs for vessels A and B were taken to provide a better representation of standards-conformant measurements for the purpose of evaluating different metrics at the shallow and intermediate depth sites. Measurements of vessel B conformed most closely to the CPA tolerances specified in ISO 17208-1 ( $-10\%$  to  $+25\%$ ).

## D. Array geometry comparisons

To compare the performance of the different hydrophone array geometries deployed during the experiment, ten measurements of each vessel were identified at each array with speeds between 20 and 21 kn (10.3–11.3 m/s) and CPA distances closest to the planned measurement track at each site. Then, the single-node and array-averaged metrics for these ten measurements were arithmetically averaged and compared to reference SLs (Fig. 7).<sup>27</sup> Standard deviations were computed for the single-node and array-averaged data to quantify the measurement repeatability (Table VII). Additionally, mean absolute residual differences between measured SLs and reference SLs were computed to quantify the reproducibility (Table VIII). Note that single-node comparisons are not shown for the M-A metric as it was only intended for use with array-averaged data. The array geometry comparisons focused on results for vessel B because this vessel had the highest quality measurements and also the greatest number of passes (see Table III). However, the

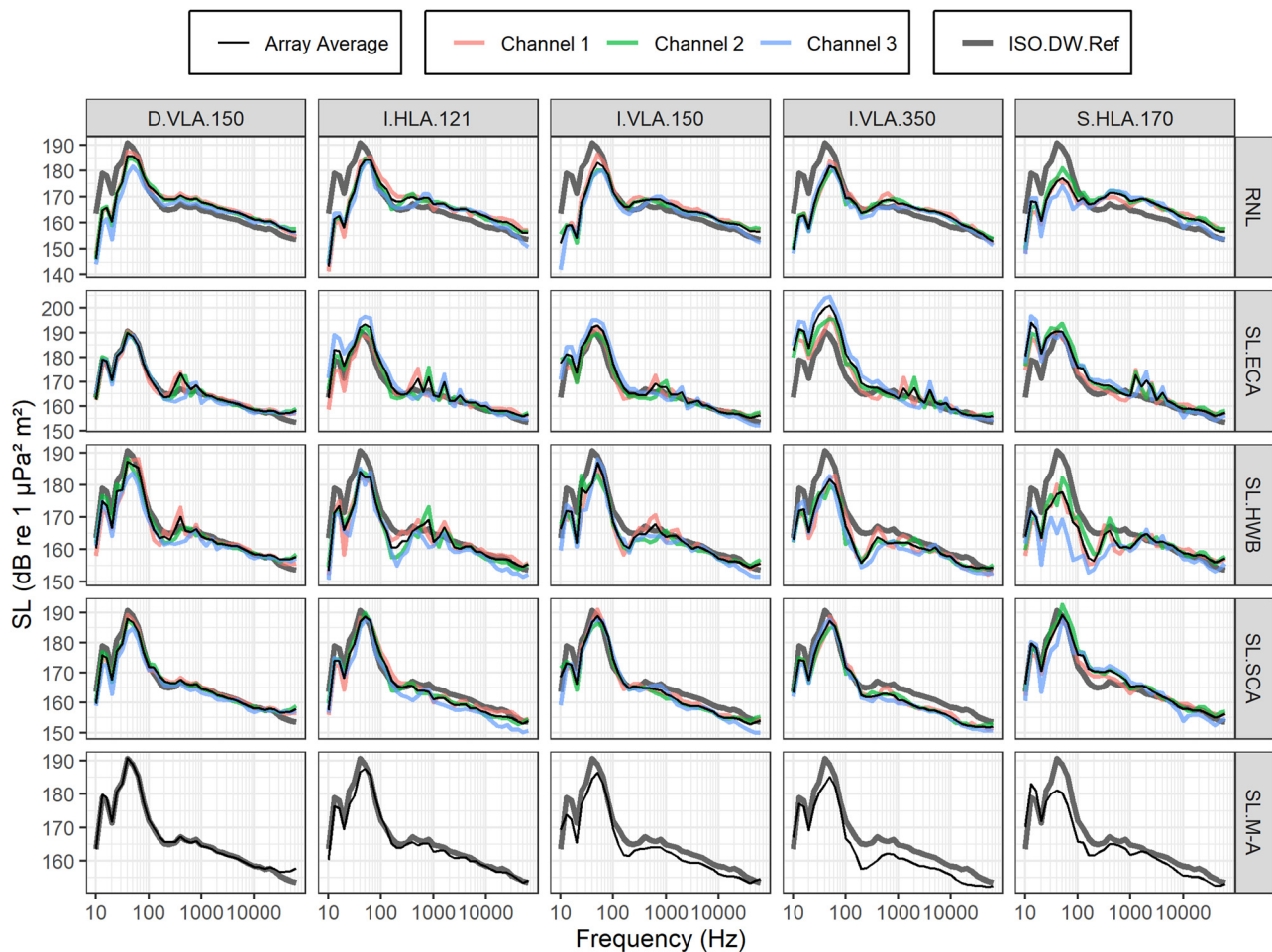


FIG. 7. (Color online) Comparisons of mean SLs for vessel B on different channels of the five hydrophone arrays: deep VLA (D.VLA.150), intermediate HLA (I.HLA.121), near intermediate VLA (I.VLA.150), far intermediate VLA (I.VLA.350), and shallow HLA (S.HLA.170). Rows correspond to different SL metrics. Each panel shows average values for the ten measurements with CPA closest to the planned distance from each array (see Fig. 3) and speeds through water between 20 and 21 kn (10.3–11.3 m/s). On the VLAs, channels 1, 2, and 3 refer to the bottom, middle, and top hydrophones, respectively. On the HLAs, channels 1, 2, and 3 refer to the nearest, middle, and farthest hydrophones from the vessel track, respectively. Colored solid lines indicate single-node values and thin black lines indicate array-average values. The thick gray line indicates the deep-water reference SL for vessel B (i.e., as shown in Fig. 6). The SL.SCA metric was calculated using the MAP SCA estimates (Fig. 5), and the SL.M-A metric was calculated using an  $\varepsilon$  coefficient of one.

TABLE VII. Standard deviations (decibels) of measured SL data for vessel *B* (20–21 kn), averaged over deep, intermediate, and shallow hydrophone arrays (30–180 m water depth). Values are calculated from data presented in Fig. 7, averaged over decidecade frequency band (10–63 000 Hz; Ref. 27).

Metric	Single node	Array average
RNL	2.14	1.51
SL.ECA	2.70	1.70
SL.HWB	2.57	1.71
SL.SCA	2.07	1.51
SL.M-A	—	1.55

results were similar for the other two vessels. As expected, array-averaged SLs differed less from the reference levels and had smaller standard deviations than the single-node SLs. This exhibited that the array-average measurements were more reproducible and repeatable than the single-node measurements. Furthermore, the VLA nodes closer to the seabed and HLA nodes closer to the vessel track matched the reference levels more closely than those near the sea surface and farther from the vessel track, respectively. This indicates that reproducibility was improved by taking measurements at shorter range and nearer to the seabed.

Generally, all of the array-averaged SL metrics (i.e., excluding RNL) did a good job of reproducing reference levels on the deep VLA (D.VLA.150) across the entire frequency range. This confirmed that the ISO deep-water measurement procedure was highly repeatable. At the intermediate site, the various metrics usually reproduced reference levels better on the two nearest arrays (I.HLA.121 and I.VLA.150) than on the one farthest array (I.VLA.350). The main issue with the array-averaged metrics at the intermediate site was underestimation of the low-frequency reference SLs, particularly, at longer ranges. On the HLA at the shallow site, reproducibility for all of the metrics was generally poorer than at the other two sites. This was especially the case for low frequencies, although the SCA and ECA metrics still appeared to reproduce reference levels reasonably well in this frequency range.

## E. Residual differences from reference SL

The reproducibility of the different metrics and array geometries was quantified by calculating statistics of the

TABLE VIII. Mean absolute residuals (decibels) between measured and reference SL data for vessel *B* (20–21 kn), averaged over deep, intermediate, and shallow hydrophone arrays (30–180 m water depth). Values are calculated from data presented in Fig. 7, averaged over decidecade frequency band (10–63 000 Hz; Ref. 27).

Metric	Single node	Array average
RNL	5.49	5.32
SL.ECA	3.26	3.28
SL.HWB	4.33	3.55
SL.SCA	2.73	2.37
SL.M-A	—	2.49

residual differences between measured decidecade band SLs and their reference values. Residuals of the decidecade band SLs were calculated for all of the URN measurements as the following difference:

$$e_i(f) = L'_{S,i}(f) - L_{S(\text{ref})}(f), \quad (30)$$

where  $L'_{S,i}(f)$  is the decidecade band SL for measurement *i* at frequency *f*, computed using any of the metrics described in Sec. II C, and  $L_{S(\text{ref})}(f)$  is the reference SL from the deep VLA for the same vessel and speed bin. For vessels *A* and *B* and speeds through water bins between 17 and 21 kn (8.8–11.3 m/s), statistics of the residuals were collected within the following three frequency ranges:

- (1) the decade band comprising 10 decidecade bands from 10 to 80 Hz (i.e., 8.91–89.1 Hz);
- (2) the decade band comprising 10 decidecade bands from 100 to 800 Hz (i.e., 89.1–891 Hz); and
- (3) the 19 decidecade bands from 1000 Hz to 63 kHz (i.e., 0.891–70.8 kHz).

Vessel C was excluded from the residual statistics as reference measurements for this vessel were of a lower grade than those for the other two study vessels. Statistics of the residuals were summarized by calculating the arithmetic mean of the absolute residuals (i.e.,  $\bar{|e_i(f)|}$ ) versus CPA bin for the array-averaged measurements (Fig. 8).<sup>27</sup>

At the deep site, all of the SLs metrics provided a reasonable match to the ISO reference levels with the best agreement, generally, for CPA ranges between 150 and 250 m. At the intermediate site, the array-average residuals appeared to show that the VLA and HLA geometries were suitable for reproducing deep-water reference measurements. The HLA geometry appeared to be slightly more robust to variations in CPA distance, but this difference was small. At the shallow site, the array measurements appeared to be less robust to CPA distance with the lowest residuals generally measured at CPA distances less than 150 m to the nearest hydrophone.

## V. DISCUSSION

### A. Geoacoustic properties

Whereas the geoacoustic inversion was expected to be a reliable technique for accurately estimating elastic properties of the seabed, the results of the inversion were likely limited to some degree by the frequency range of PL data (500–1200 Hz) compared to the frequency range of the vessel URN data (10–63 000 Hz). This is because the ability of test signals to probe the seabed is dependent on frequency with lower-frequency signals able to probe to deeper depths and higher-frequency signals able to probe with finer spatial resolution. Although the posterior probability distribution (PPD) was not available for this study, it is probable that the uncertainty of geoacoustic properties increases with depth below the seafloor. The MAP model can be relatively far from the majority of the probability indicated by the PPD,

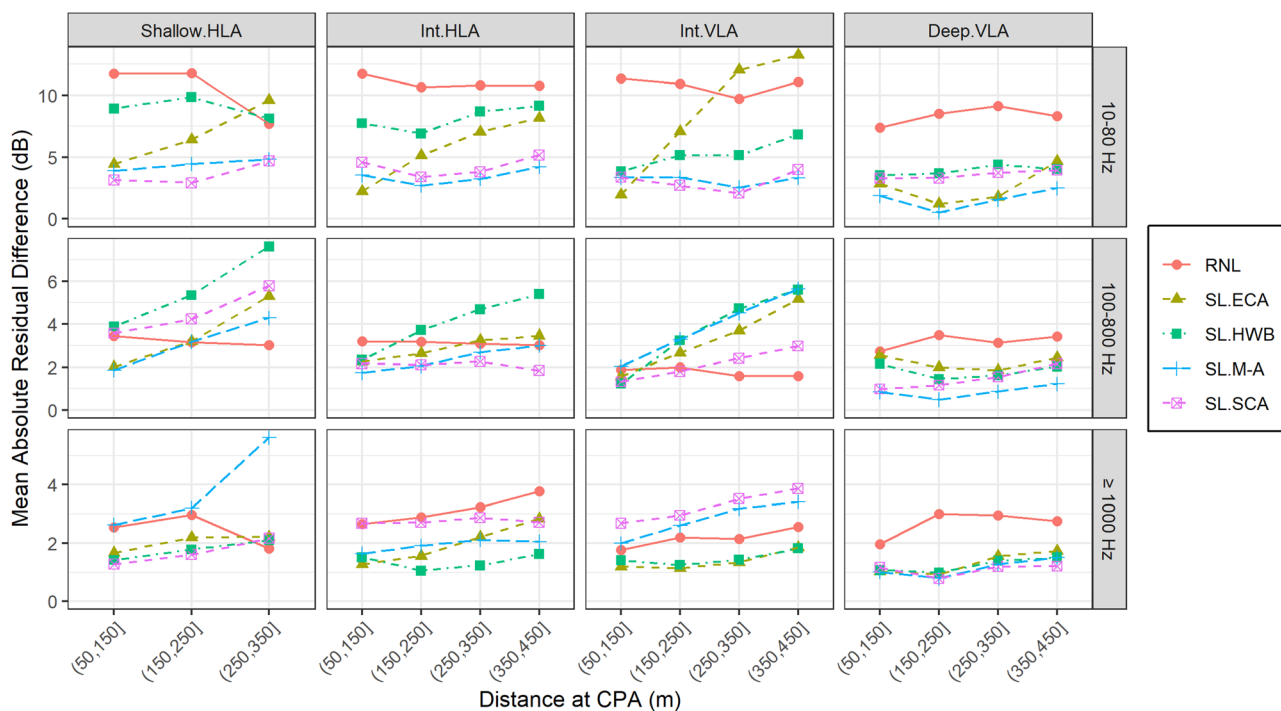


FIG. 8. (Color online) Mean absolute residual differences of array-averaged SL metrics from their reference values versus CPA distance (100 m bins). Columns show different arrays and rows show different decidecade band ranges. The SL.SCA metric was calculated using the MAP SCA estimates (Fig. 5), and the SL.M-A metric was calculated using an  $\varepsilon$  coefficient of one.

which would lead to errors in low-frequency PL. Another possible source of error at the shallow site was that geoacoustic properties were obtained from an inversion that considered the slope of the seabed, whereas the seabed was considered flat (i.e., range-independent) when calculating the various SL metrics.

The relatively high mismatch of the HWB metric below 1000 Hz at the intermediate and shallow sites suggested that the MAP geoacoustic properties may have underestimated bottom loss at lower frequencies. Nevertheless, the critical angles estimated from the MAP profiles did not appear to affect the SCA metric to the same degree. Furthermore, there could be other reasons why the wavenumber integration model underestimated PL. For example, Wales and Heitmeyer<sup>17</sup> found that using a monopole source representation in their PL model introduced artifacts into their source spectrum estimates, which led them, instead, to use a Gaussian source-depth distribution. A more detailed analysis would be needed to determine how sensitive the HWB method was to variations in the seabed geoacoustic properties and assumed source depth. It also may be possible to directly invert geoacoustic properties using vessel URN data as demonstrated by Tollefson *et al.*<sup>29</sup>

## B. Effect of environmental mismatch

Limited knowledge of the environment is usually the greatest source of uncertainty when measuring URN in shallow water. Furthermore, the detailed PL inversion approach used for measuring seabed properties in the MMP2

experiment is impractical for most real-world applications. Although some knowledge of seabed properties is required for measuring URN in shallow water, in most circumstances, such properties would be estimated from a qualitative description of the seabed geology based on tables<sup>30</sup> or models.<sup>31,32</sup> Such estimates are liable to introduce additional uncertainty into the measured SLs.

The effect of environmental mismatch on the SCA and M-A SL metrics was investigated by adjusting parameters related to the influence of the seabed on PL. With the SCA metric, the influence of the seabed is determined by the critical angle parameter,  $\psi$ . Three different  $\psi$  parameters were evaluated for the SCA metric:

- (1) the MAP estimate of the frequency-dependent critical angle,  $\psi(f)$ , as determined by the geoacoustic inversion procedure (see Fig. 5), and this was the baseline value;
- (2) a frequency-independent critical angle,  $\psi = 33.4^\circ$ , representing a homogeneous sand seabed with medium grain size ( $1.5 \phi$ ) and a sound speed ratio of  $c_p/c_w = 1.1978$ ; and
- (3) a frequency-independent critical angle,  $\psi = 17.4^\circ$ , representing a homogeneous silt seabed with medium grain size ( $5.5 \phi$ ) and a sound speed ratio of  $c_p/c_w = 1.0479$ .

Note that the latter two  $\psi$  values bracket the range of critical angles ( $22.5^\circ$ – $30.4^\circ$ ), which would have been estimated from the measurements of Pignot and Chapman,<sup>28</sup> taken in nearby Haro Strait, which were the best available source of information on seabed properties in the study area prior to the MMP2 experiment.

With the M-A metric, the influence of the seabed is determined by the parameter,  $\varepsilon$ , which may be adjusted to represent a soft or hard seabed. Two different  $\varepsilon$  values were evaluated for the M-A metric:

- (1) a value of  $\varepsilon = 1$ , representing a soft sand seabed, and this was the baseline value; and
- (2) a value of  $\varepsilon = 2$ , representing a hard basalt seabed.

SLs computed using the different seabed parameters were compared on each of the five different line arrays using URN measurements between 20 and 21 kn (10.3–11.3 m/s) for vessel *B* within a fixed range of CPA distances (Fig. 9).

For the SCA metric, SLs were insensitive to environmental mismatch on the deep VLA, which was consistent with the expectation that the seabed's influence on PL is weak in deep water. The seabed type was more influential at the intermediate site, where environmental mismatch appeared to have a greater influence at longer CPA distances (i.e., on I.VLA.350). Interestingly, low-frequency mismatch on the intermediate arrays was improved for the silt  $\psi$  parameter compared to the MAP estimate, although this was not the case at higher frequencies. Sensitivity of the SCA metric to environmental mismatch appeared to be greatest at the shallow HLA, and the alternate  $\psi$  values did not appear to improve the mismatch at this site.

For the M-A metric, SLs were equally sensitive to environmental mismatch on all of the line arrays and at all of the sites. This was expected because the influence of the  $\varepsilon$  parameter does not explicitly depend on source-receiver geometry or water depth. In this regard,  $\varepsilon$  behaves more as an empirical parameter rather than a physical parameter. The  $\varepsilon = 2$  seabed model did not improve the mismatch of the M-A SL estimates on any of the arrays, but this represents a basalt seabed type (i.e., with compressional-wave speed of 5.25 km/s), which was significantly different from the inverted seabed properties at the three test sites.

### C. Hydrophone geometry

The experimental data suggested that HLAs and VLAs were suitable for obtaining consistent SL measurements in water depths less than 100 m over a wide range of frequencies. One advantage of horizontal arrays, however, was that they were not susceptible to knock-down due to ocean currents. Interestingly, the M-A metric performed well for the horizontal array geometry (particularly, at the intermediate site), even though it was developed for a vertical array of hydrophones. In terms of distance from the vessel track, some metrics performed best at shorter CPA distances (ECA and HWB), whereas other metrics performed well over a wide range of CPA distances (SCA and M-A). However, comparison of array data from the intermediate site suggested that the two closer line arrays (with 121 and 150 m nominal CPA distance) had overall lower mismatch than the farthest array (with 350 m nominal CPA distance) when considering a wide range of metrics. These results suggest that some flexibility in array geometry is possible when performing vessel URN measurements.

Single-node measurements suggested that performance of many of the metrics was best when hydrophones were 50–150 m from the vessel track. Interestingly, within this CPA distance, some of the single-node metrics (ECA and SCA) performed comparably well to their array-averaged counterparts, particularly, for nodes on or near the seabed. This suggests that with favourable geometry, single-node URN measurements are an acceptable alternative to array-average URN measurements when a slightly lower grade of measurement is acceptable (e.g., as in Grade C of the ANSI standard S.12–64). Nevertheless, there is a trade-off with temporal averaging time versus CPA distance (averaging time is proportional to CPA distance), as well as the desire to avoid measuring URN in the near field of the vessel.

The results of this experiment indicate that reproducible measurements can be obtained when the CPA distance is shorter than the minimum distance specified by the current

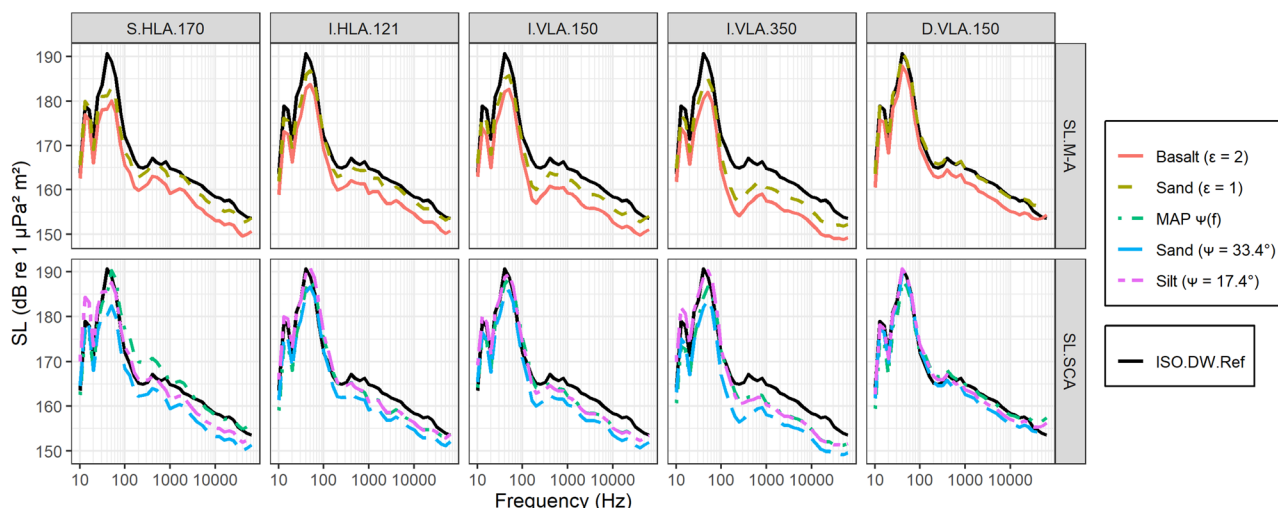


FIG. 9. (Color online) Examination of the effect of environmental mismatch on the SCA and M-A SL metrics for measurements of vessel *B* with speeds between 20 and 21 kn (10.3–11.3 m/s). Columns show different arrays and rows show different metrics.

standard (i.e., at CPA distances of less than one vessel length and as close as 50 m to the source, in this case). This suggests that the important noise-generating sources on vessels A–C (e.g., the propellers and engine room) were likely separated by distances shorter than their overall vessel length. Nonetheless, measurements in the acoustic near field (i.e., where source-receiver propagation ranges are significantly different for important noise-generating sources on the vessel) should be avoided.

#### D. Reproducibility and repeatability of SLs

The purpose of following a standard methodology when performing vessel URN measurements is to ensure that the reported SLs are repeatable and reproducible. For the current experiment, repeat passes of vessels A–C were performed over 3 months under different loading, operating, and weather conditions. While this likely led to greater variability in measured SLs than would be observed under a strictly standards-conformant test procedure (i.e., following the strict test sequence described in ISO standard 17208–1), analysis of the standard deviations suggested that a repeatability  $\pm 1.5$  dB is achievable for the best performing metrics (Table VII). Furthermore, residual differences between the best performing metrics and the ISO deep-water reference SLs suggested that a reproducibility of  $\pm 2.5$  dB is achievable between deep and shallow URN measurements (Table VIII).

Variance in the URN measurements was reduced experimentally by binning them into narrow speed ranges and CPA distances (i.e., controlling for repeatability) and then averaging several measurements inside these bins. Nonetheless, some degree of uncertainty remained in the resulting SL estimates due to uncontrollable experimental factors. These uncertainties were consistent with prior observations by Vendittis and Arveson,<sup>4</sup> who suggested that controlled vessel SL measurements are unlikely to achieve better than 1 dB of repeatability, even under optimal circumstances.

One aspect of uncertainty, which was not addressed by the current study, is how the choice of source depth ( $d$ ) affects the reproducibility of estimated SLs. Because the calculation is sensitive to source depth, ISO standard 17208–2 specifies a value equal to 70% of the vessel draft at the time of measurement. However, the effect of this specific choice on the reproducibility of the estimated SLs is unknown, and it remains possible that another choice (e.g., based on the propeller geometry, as in Gray and Greeley<sup>33</sup>) may produce more accurate estimates. Another aspect of SL variability that is not addressed by existing standards is fore/aft directivity of vessel noise emissions. Fore/aft directivity of SLs has been well documented for large vessels,<sup>14,34,35</sup> although reasons for this variability are less well understood. The existing standards focus on beam-aspect noise emissions by averaging within a 60° broadside window, but some directivity is possible even inside this range of angles.

#### E. Robustness of metrics

Robustness is a desirable property of a SL metric, which means that errors in estimated SLs should be insensitive to reasonable uncertainties in environmental conditions and source-receiver geometry. A metric that provides a robust measurement may be preferred to one that does not, even if that means that the robust metric has lower precision when measurement conditions are known precisely. The experimental data from this study showed that no single SL metric performed best over all of the water depths, array geometries, CPA distances, and frequency ranges. However, a robust metric should perform well over a wide range of measurement conditions and not just over a narrow range of conditions. This is particularly true when uncertainty in seabed geoacoustic properties is concerned as these are difficult to measure reliably without considerable effort. Robustness across CPA ranges is also desirable in shallow water because the bathymetry restricts the distances at which hydrophones can be positioned to measure specific receiver angles. Generally, standards, such as ISO 17208–1, ensure reproducibility by limiting allowable CPA distances to an optimal range during URN measurements.

Of the metrics evaluated during this experiment, the SCA and M-A metrics appeared to be the most robust overall. These metrics both performed well at longer CPA distances compared to the other metrics, although the array geometry comparisons (see Sec. IV D) suggested that the SCA metric better reproduced low-frequency SLs at the shallow site. The robustness of these metrics was likely the result of their inclusion of knowledge of the acoustic properties of the seabed (i.e., as measured using geoacoustic inversion), although they did so in different ways. In shallow water, accounting for the influence of the seabed is more important at longer CPA distances. By contrast, the ECA metric reproduced reference levels satisfactorily at short range but had larger errors at longer CPA distances.

The HWB metric was not robust at low frequency, where it struggled to produce consistent SL estimates at longer CPA distances. The relatively poor performance of the HWB metric was surprising given the sophistication of the method. One possibility is that the results of the geoacoustic inversion were too sensitive to the specific frequency range of the PL measurements (i.e., the PL model may have been overtuned to the PL data). Another possibility is that the errors were caused by the point-source assumption, and estimates would be improved by using a distribution of source depths. Regardless of the explanation, the experimental results suggested that the HWB metric was not as robust as the other methods below 1000 Hz.

An aspect of robustness that was not evaluated during the field trials was sensitivity to estimated source depth. It is well known that low-frequency SLs are very sensitive to errors in estimated source depth, which is one reason for the prevalence of RNL when reporting vessel URN measurements. However, vessels A–C only had very small variations

in logged draft (within  $\pm 20$  cm) during the experiment, making sensitivity to source depth difficult to evaluate.

## VI. CONCLUSIONS

Repeated vessel noise measurements, performed over a period of 3 months in British Columbia's Southern Gulf Islands, yielded valuable data to inform experimental methods for performing shallow-water vessel URN measurements. Measurements of three anonymized vessels (denoted *A*, *B*, and *C*), were collected on five moored hydrophone arrays, deployed in three different water depths. These measurements confirmed that it was possible to obtain reproducible vessel SL estimates in shallow water with only a moderate increase in complexity beyond methods codified in existing ISO standards. Nonetheless, the reproducibility of SLs measured in shallow water may be limited to some extent by knowledge of the acoustic properties of the seabed.

The following four SL metrics were evaluated using experimental data from this study, reflecting four different approaches to analyzing vessel URN measurements. These methods were evaluated by comparing them with the ISO method for measuring deep water SLs from ISO 17208:

- (1) HWB method: This is a method for estimating PL of an URN measurement in any water depth using a hybrid model based on low-frequency wavenumber integration and high-frequency beam tracing. This method requires a detailed description of the acoustic properties of the environment (assumed to be range-independent) and sophisticated numerical models. The PL estimate from the numerical models is used to calculate a monopole SL directly from the URN data;
- (2) ECA method: This is a method for calculating PL for an URN measurement performed at any grazing angle but which neglects the influence of the seabed. This method is similar in principle to the ISO method, but it does not assume a fixed set of grazing angles and is based on an exact Lloyd's-mirror PL calculation, integrated over decidecade frequency bands;
- (3) SCA method: This is a method for calculating SLs from single-node RNL measurements in any water depth by applying physics-based correction factors to account for the critical angle of the seabed (which must be known or estimated) and water depth. While in this study the critical angle was estimated using a geoacoustic inverse method, the critical angle could be calculated using a simple formula (see Table I) at locations with a uniform seabed. When applied to URN measurements on an array, this method can be averaged over multiple hydrophone nodes (i.e., at different grazing angles) to yield a higher-precision SL estimate; and
- (4) M-A method: This is a method for calculating SLs from array-averaged RNL measurements in shallow water by applying an empirical correction formula to account for the frequency-dependent influence of the seabed and water depth. This method includes an empirical

parameter ( $\varepsilon$ ), which is selected according to the seabed type (which must be known). This method was developed for a vertical array of three hydrophones spanning the water column.

Of these four metrics, M-A and SCA provided the most robust SL estimates over a wide range of frequencies and water depths while accounting for the influence of the seabed on URN measurements. Both metrics gave array-averaged SLs that were repeatable to within  $\pm 1.5$  dB (standard deviation). Furthermore, these two metrics reproduced reference SLs comparably well between deep- and shallow-water sites ( $\pm 2.5$  dB mean residual difference), although the SCA method appeared to perform better at 30 m depth (where an HLA was deployed rather than the VLA assumed by the M-A method). As expected, uncertainty regarding the seabed properties affected the accuracy of both of these methods.

Of the remaining two metrics, the ECA method reproduced deep-water reference SLs well at short CPA distances but not at longer CPA distances. The HWB method reproduced reference levels well at high frequencies (1000 Hz and above), but it had difficulty at lower frequencies and longer CPA distances. The reasons for the poor robustness of the HWB method are not yet clear, but they may have been related to the relatively narrow frequency range of PL data (500–1200 Hz) used to tune the geoacoustic parameters in the HWB model. This is a possible topic for future investigation.

Experimental data indicated that HLA and VLA geometries were effective for reproducing reference SLs in intermediate (approximately 70 m) and shallow (approximately 30 m) water depths, provided that they sampled a range of grazing angles. The experimental results at the shallow and intermediate sites suggested that single-node measurements may be used to reproduce SL estimates that are consistent with the ISO deep-water standard (albeit with slightly greater measurement error), provided that the hydrophone is deployed at the seabed close to the source (50–150 m range). The experimental results also suggested that it was possible to obtain repeatable SL measurements at CPA distances closer than one vessel length from the source (although it remains important to avoid the near field). Such measurement geometries may be advantageous in shallow water, where bottom loss makes accurate SL measurements difficult at longer CPA distances and surface cancellation makes accurate SL measurements difficult at shallow grazing angles.

## ACKNOWLEDGMENTS

Carmen Lawrence, Jennifer Wladichuk, Graham Warner, Connor Grooms, and Calder Robinson (JASCO) performed the deployments and retrievals of the hydrophone arrays during the British Columbia field measurements. Captain Greg Bellavance and the crews of *M/V Moving Experience* and *M/V Celtic V* provided vessel support during the British Columbia field measurements. Jason Hines, Julien Delarue, and Eric Lumsden (JASCO) carried

out field tests in Halifax Harbour to refine the designs of the hydrophone moorings. Members of JASCO's hardware engineering team, led by Steve Fenton, tested, assembled, and shipped the hydrophone systems used in the experiment. Max Schuster and Dietrich Wittekind (DW-ShipConsult) contributed to development of the experimental design and data analysis methods. Federica Pace and Terry Deveau (JASCO) carried out sound propagation and SL analysis to support development of the experimental design. The members of ISO working group ISO/TC 43/SC 3/WG 1, led initially by Stephen Robinson (National Physical Laboratory) and later by Christ de Jong (TNO), provided feedback on the experimental plan. Veronique Nolet and Laurence Lecavalier (Transport Canada) provided input on the experimental design and feedback on the draft manuscript. Valentin Meyer (Naval Group) provided helpful guidance on the implementation of the M-A SL formulas applied in this work. We would also like to acknowledge the contribution of two anonymous peer reviewers, whose helpful feedback improved the quality of the final manuscript. This work was funded by the Government of Canada.

<sup>1</sup>ISO 17208-1:2016, “Underwater acoustics—Quantities and procedures for description and measurement of underwater sound from ships—Part 1: Requirements for precision measurements in deep water used for comparison purposes” (International Organization for Standardization, Geneva, Switzerland, 2019), available at <https://www.iso.org/standard/62408.html> (Last viewed 23 February 2023).

<sup>2</sup>ISO 17208-2:2019, “Underwater acoustics—Quantities and procedures for description and measurement of underwater sound from ships—Part 2: Determination of source levels from deep water measurements” (International Organization for Standardization, Geneva, Switzerland, 2019), available at <https://www.iso.org/standard/62409.html> (Last viewed 23 February 2023).

<sup>3</sup>ANSI S12.64-2009, *American National Standard: Quantities and Procedures for Description and Measurement of Underwater Sound from Ships—Part 1: General Requirements* (American National Standards Institute and Acoustical Society of America, New York, 2009), available at [https://webstore.ansi.org/Standards/ASA/ANSIASAS12642\\_009Part](https://webstore.ansi.org/Standards/ASA/ANSIASAS12642_009Part) (Last viewed 23 February 2023).

<sup>4</sup>D. J. Vendittis and P. T. Arveson, “Ten challenges in measuring and reporting ship noise levels,” *JASA Express Lett.* **2**(3), 036801 (2022).

<sup>5</sup>A. Brooker and V. Humphrey, “Measurement of radiated underwater noise from a small research vessel in shallow water,” *Ocean Eng.* **120**, 182–189 (2016).

<sup>6</sup>V. Meyer and C. Audoly, “A parametric study of the environment and the array configuration for underwater noise measurement from ships in shallow water,” in *26th International Congress on Sound and Vibration*, 7–11 July 2019, Montreal, Canada, pp. 1–8.

<sup>7</sup>M. A. Ainslie, S. B. Martin, K. B. Trounce, D. E. Hannay, J. M. Eickmeier, T. J. Deveau, K. Lucke, A. O. MacGillivray, V. Nolet, and P. Borys, “International harmonization of procedures for measuring and analyzing of vessel underwater radiated noise,” *Mar. Pollut. Bull.* **174**, 113124 (2022).

<sup>8</sup>ANSI/ASA S12.64 does not use the term RNL and instead refers to this quantity as “affected source level” or simply “source level.” We have adopted the ISO terminology here for clarity.

<sup>9</sup>A. O. MacGillivray, S. B. Martin, J. N. Dolman, Z. Li, G. A. Warner, C. B. Lawrence, F. Pace, M. Schuster, and D. Wittekind, “Towards a standard for vessel URN measurement in shallow water,” Technical Report, Document No. 02167, version 2.0, JASCO Applied Sciences (2021).

<sup>10</sup>ISO 18405:2017, “Underwater acoustics—Terminology” (International Organization for Standardization, Geneva, Switzerland, 2017), available at <https://www.iso.org/standard/62406.html> (Last viewed 23 February 2023).

<sup>11</sup>M. A. Ainslie, M. B. Halvorsen, and S. P. Robinson, “A terminology standard for underwater acoustics and the benefits of international standardization,” *IEEE J. Ocean. Eng.* **47**(1), 179–200 (2022).

<sup>12</sup>IEC 61260-1:2014, “Electroacoustics—Octave-band and fractional-octave-band filters—Part 1: Specifications” (International Electrotechnical Commission, Geneva, Switzerland, 2014), available at <https://webstore.iec.ch/publication/5063> (Last viewed 23 February 2023).

<sup>13</sup>M. A. Ainslie, J. L. Miksis-Olds, S. B. Martin, K. D. Heaney, C. A. F. de Jong, A. M. von Benda-Beckmann, and A. P. Lyons (2018). “ADEON underwater soundscape and modeling metadata standard,” *Technical Report version 1.0, ADEON Prime Contract No. M16PC00003*, JASCO Applied Sciences, 35 pp.

<sup>14</sup>M. Gassmann, S. M. Wiggins, and J. A. Hildebrand, “Deep-water measurements of container ship radiated noise signatures and directionality,” *J. Acoust. Soc. Am.* **142**(3), 1563–1574 (2017).

<sup>15</sup>F. B. Jensen, W. A. Kuperman, M. B. Porter, and H. Schmidt, “Computational ocean acoustics,” in *AIP Series in Modern Acoustics and Signal Processing*, 2nd ed. (AIP-Springer, New York, 2011), 794 pp.

<sup>16</sup>M. B. Porter and Y. C. Liu, “Finite-element ray tracing,” in *International Conference on Theoretical and Computational Acoustics*, edited by D. Lee and M. H. Schultz (World Scientific, Singapore, 1994), Vol. 2, pp. 947–956.

<sup>17</sup>S. C. Wales and R. M. Heitmeyer, “An ensemble source spectra model for merchant ship radiated noise,” *J. Acoust. Soc. Am.* **111**(3), 1211–1231 (2002).

<sup>18</sup>A. O. MacGillivray, Z. Li, D. E. Hannay, K. B. Trounce, and O. Robinson, “Slowing deep-sea commercial vessels reduces underwater radiated noise,” *J. Acoust. Soc. Am.* **146**, 340–351 (2019).

<sup>19</sup>P. Jiang, J. Lin, J. Sun, X. Yi, and Y. Shan, “Source spectrum model for merchant ship radiated noise in the Yellow Sea of China,” *Ocean Eng.* **216**, 107607 (2020).

<sup>20</sup>M. A. Ainslie and J. G. McColm, “A simplified formula for viscous and chemical absorption in sea water,” *J. Acoust. Soc. Am.* **103**(3), 1671–1672 (1998).

<sup>21</sup>M. A. Ainslie, P. H. Dahl, C. A. F. de Jong, and R. M. Laws (2014). “Practical spreading laws: The snakes and ladders of shallow water acoustics,” in *UA2014—2nd International Conference and Exhibition on Underwater Acoustics*, 22–27 June 2014, Island of Rhodes, Greece, pp. 879–886.

<sup>22</sup>V. Meyer and C. Audoly, “Accounting for sea floor properties in the assessment of underwater noise radiated from ships in shallow water,” *Proc. Mtgs. Acoust.* **40**(1), 070007 (2020).

<sup>23</sup>M. A. Ainslie, D. E. Hannay, A. O. MacGillivray, K. B. Trounce, and K. Lucke, “Proposed alignment of measurement and analysis procedures for quiet ship certifications.” Technical memorandum, Document Number 02024, version 9.0 for Vancouver Fraser Port Authority (VFPA), JASCO Applied Sciences (2021).

<sup>24</sup>D. E. Hannay, X. Mouy, and Z. Li, “An automated real-time vessel sound measurement system for calculating monopole source levels using a modified version of ANSI/ASA S12.64-2009,” *Can. Acoust.* **44**(3), 166–167 (2016).

<sup>25</sup>E. Baudin and H. Mumm, “Guidelines for regulation on UW noise from commercial shipping (SONIC Deliverable 5.4),” in *Achieve Quieter Oceans by Shipping Noise Footprint Reduction*, FP7-Grant agreement No. 2015, Vol. 314227 (2015).

<sup>26</sup>F. Traverso, T. Gaggero, E. Rizzato, and A. Trucco, “Spectral analysis of the underwater acoustic noise radiated by ships with controllable pitch propellers,” in *Oceans 2015*, 18–21 May 2015, Genova, Italy, pp. 1–6.

<sup>27</sup>See supplementary material at <https://www.scitation.org/doi/suppl/10.1121/10.0017433> for a description of the methods used for inverting geoacoustic properties at the measurement sites; plots of residual differences of measured source levels from deep water reference levels in Fig. S.1; additional statistics of the residual differences in Figs. S.3–S.5; for an expanded presentation of standard deviation versus frequency band data in Fig. S.2; and an expanded presentation of mean absolute residual differences versus frequency band data in Fig. S.1.

<sup>28</sup>P. Pignot and N. R. Chapman, “Tomographic inversion of geoacoustic properties in a range-dependent shallow-water environment,” *J. Acoust. Soc. Am.* **110**(3), 1338–1348 (2001).

<sup>29</sup>D. Tollefson, W. S. Hodgkiss, S. E. Dosso, J. Bonnel, and D. P. Knobles, “Probabilistic estimation of merchant ship source levels in an uncertain shallow-water environment,” *IEEE J. Ocean. Eng.* **47**(3), 647–656 (2022).

- <sup>30</sup>M. A. Ainslie, *Principles of Sonar Performance Modeling* (Praxis Books, Springer, Berlin, 2010).
- <sup>31</sup>E. L. Hamilton, “Geoaoustic modeling of the sea floor,” *J. Acoust. Soc. Am.* **68**(5), 1313–1340 (1980).
- <sup>32</sup>M. J. Buckingham, “Compressional and shear wave properties of marine sediments: Comparisons between theory and data,” *J. Acoust. Soc. Am.* **117**, 137–152 (2005).
- <sup>33</sup>L. M. Gray and D. S. Greeley, “Source level model for propeller blade rate radiation for the world’s merchant fleet,” *J. Acoust. Soc. Am.* **67**(2), 516–522 (1980).
- <sup>34</sup>P. T. Arveson and D. J. Venditti, “Radiated noise characteristics of a modern cargo ship,” *J. Acoust. Soc. Am.* **107**(1), 118–129 (2000).
- <sup>35</sup>M. Mustonen, A. Klauson, J. Laanearu, M. Ratassepp, T. Folegot, and D. Clorennec, “Passenger ship source level determination in shallow water environment,” *Proc. Mtgs. Acoust.* **27**(1), 070015 (2016).
- <sup>36</sup>L. M. Brekhovskikh, “Waves in layered media,” in *Applied Mathematics and Mechanics*, 2nd ed. (Academic, New York, 1980), Vol. 16, 503 pp.
- <sup>37</sup>CHS, “Canadian Hydrographic Service non-navigational (NONNA) bathymetric data,” 2021. (Department of Fisheries and Oceans, Ottawa, Canada), available at <https://open.canada.ca/data/en/dataset/d3881c4c-650d-4070-bf9b-1e00aabf0a1d> (Last viewed 25 May 2022).
- <sup>38</sup>M. A. Ainslie and M. A. Wood, “Semi-coherent image method to estimate propagation loss in shallow water for measuring surface vessel source level,” *Proc. Mtgs. Acoust.* **47**(1), 070024 (2023).